



Unequal termination impedance parallel-coupled lines band-pass filter with arbitrary image impedance

Phirun Kim, Girdhari Chaudhary & Yongchae Jeong

To cite this article: Phirun Kim, Girdhari Chaudhary & Yongchae Jeong (2018) Unequal termination impedance parallel-coupled lines band-pass filter with arbitrary image impedance, Journal of Electromagnetic Waves and Applications, 32:8, 984-996, DOI: [10.1080/09205071.2017.1411837](https://doi.org/10.1080/09205071.2017.1411837)

To link to this article: <https://doi.org/10.1080/09205071.2017.1411837>



Published online: 18 Dec 2017.



Submit your article to this journal [↗](#)



Article views: 21




View related articles [↗](#)



View Crossmark data [↗](#)



Unequal termination impedance parallel-coupled lines band-pass filter with arbitrary image impedance

Phirun Kim , Girdhari Chaudhary  and Yongchae Jeong 

Division of Electronics and Computer Engineering, IT Convergence Research Center, Chonbuk National University, Jeonju-si, Republic of Korea

ABSTRACT

This paper presents an analytical design for a microstrip parallel-coupled line bandpass filter (BPF) with arbitrary termination and image impedances. Using the proposed design formulas, multistage arbitrary termination impedance BPFs can be designed with a very high impedance transforming ratio (r). The fractional bandwidth and return losses are maintained even though the r and image impedance are varied. To validate the design formulas, two- and three-stage BPFs are fabricated and measure at the center frequency (f_0) of 2.6 GHz. The filter 1 and filter 2 are designed with termination impedances of 50–300 Ω and 20–50 Ω , respectively. The measured results of both filters show a good agreement with the simulations. The measured passband insertion and return losses of filter 1 are better than 0.8 and 19.6 dB, respectively. Similarly, the measured passband insertion and return losses of filter 2 are better than 1.5 and 19 dB, respectively.

ARTICLE HISTORY

Received 3 July 2017
Accepted 25 November 2017

KEYWORDS

Arbitrary termination bandpass filter; image impedance; J -inverter; parallel-coupled line

1. Introduction

The bandpass filter (BPF) with an arbitrary termination impedance was analyzed and designed to use in modern wireless communication systems in order to reduce the circuit size, loss, complex circuit, and provide an out-of-band suppression. The general parallel-coupled line BPFs were analyzed and designed with equal termination impedances (i.e. 50–50 Ω) [1–5]. In [1], the first parallel-coupled line BPF was synthesized by S.B. Cohn for the Chebyshev and Butterworth responses. The design formulas were derived and applicable for equal termination impedance coupled resonator filters. In [2,3], an analysis and optimization of parallel-coupled line BPF were derived for an arbitrary characteristic image impedance of coupled lines, but the arbitrary termination impedance of source and load impedance was not discussed. The modified parallel-coupled line BPFs by adding defected ground structure (DGS) and shunt stubs were discussed in [4] and [5] with wide-stopband characteristics. In [6], a new design formulas of wideband parallel-coupled line BPF was derived up to nine stages ($n = 9$) based on a composite $ABCD$ matrices. The BPF with alternative J/K inverters was proposed in [7] with wide stopband characteristics. However, these conventional design equations were only applicable for even-order Chebyshev responses BPF with

equal termination impedances. Wideband and balanced BPFs using multiple stub TLs and coupled lines were presented in [8]. Moreover, substrate integrate waveguide and microstrip line dual-band BPFs were presented in [9,10], respectively, with equal termination impedance. The general design formulas of equal termination impedance of wideband, single-band, and dual-band BPFs have been derived, but the general solutions for unequal termination impedance BPFs were not solved.

An impedance transformer (IT) is one of the arbitrary termination impedance circuits. Indeed, a quarter-wavelength IT was widely used; however, this network has some limitations such as difficulty in realization for very high impedance transforming ratio (r) [11] and poor out-of-band suppression [12]. To overcome such limitations, various types of coupled line ITs have been proposed [13–20]. In [13], a single open-circuit coupled line with a predefined coupling coefficient was introduced as the IT. In [14]–[16], a coupled line IT with a shunt stub TL and its application with a power divider and power amplifier were demonstrated. The shunt open-circuit stub TL was used to produce transmission zeros in the stopband and to enhance the passband bandwidth. In [17], a dual-band filtering power divider with unequal termination impedance was designed based on the matching ladder network of [18] with a limited of r (i.e. $0.5 < r < 2$). To enhance selectivity and r , two cascade parallel-coupled line IT was proposed in [19]. In [20], a multi-section parallel-coupled line BPF with unequal termination impedance was presented, and times consuming is needed for the optimization process. Furthermore, the impedance transforming ratio is low.

Another application of unequal termination impedance filters were presented in [21–26]. In [21], the input- and output-matching networks of the amplifier were designed in microstrip line by optimizing from the low-pass filter of [22]. Moreover, the BPFs with one [23], two [24], and three [25] poles were analyzed from the coupling matrix to directly match with the output impedance of the amplifier. The power amplifier was designed on the microstrip line; however, the filter was designed with evanescent-mode cavities resonator. The co-design method might reduce the circuit size and obtained a high efficiency. Furthermore, the synthesis approach of the coupling matrix with arbitrary termination impedance was briefly explained in [26] without any fabrication of the validations.

In this paper, the general design formulas of the arbitrary termination impedance BPFs are derived using parallel-coupled lines structure. The design formulas provide more accurately and faster design and can be used to calculate the n -resonators, the arbitrary termination impedances, and the arbitrary characteristic image impedance of the coupled lines. Using the proposed design equations, the coupling coefficients of arbitrary termination impedance coupled line BPF can be controlled by changing image impedance of coupled lines, while the conventional design equations were only applicable for equal termination impedance BPF with fixed characteristic image impedance (typically termination impedance of $50\ \Omega$). To validate the design formulas, two BPFs with termination impedances of $50\text{--}300$ and $20\text{--}50\ \Omega$ are fabricated on a microstrip line at the design center frequency of $2.6\ \text{GHz}$. The measured performances of both filters show very good agreement with specifications. For filter 1, the measured passband insertion and input/output return loss are better than 0.8 and $19.6\ \text{dB}$, respectively. For filter 2, the measured passband insertion and input/output return loss are better than 1.5 and $19\ \text{dB}$, respectively.

2. Circuit analysis

Figure 1 shows the proposed structure of multi-stage parallel-coupled line BPF with different even- and odd-mode impedances, where the termination admittances of source and load are G_S and G_L . The electrical lengths of all coupled lines are set to be θ . Figure 2 shows a parallel-coupled line section and its equivalent circuit [27]. By equating the ABCD matrix of the parallel-coupled line and its equivalent circuit, the even- and odd-mode characteristic impedances are derived as mentioned [27]. In more general, the even- and odd-mode impedances are written as (1):

$$(Z_{0e})_{i+1} \Big|_{i=0 \text{ to } n} = Z_1 (1 + J_{i,i+1} Z_1 + J_{i,i+1}^2 Z_1^2) \tag{1a}$$

$$(Z_{0o})_{i+1} \Big|_{i=0 \text{ to } n} = Z_1 (1 - J_{i,i+1} Z_1 + J_{i,i+1}^2 Z_1^2). \tag{1b}$$

From the relationship of Figure 2(a) and (b), the equivalent circuit of Figure 1 is depicted in Figure 3(a). From Figure 3(a), in case the G_S is not equal to the Y_1 , the input admittance (Y_{01}) looking into the source is obtained as (2). $Y_1 = 1/Z_1$ is the image admittance of parallel-coupled line.

$$Y_{01} = Y_1 \frac{G_S + jY_1 \tan \theta}{Y_1 + jG_S \tan \theta} \approx Y_1 \left[\frac{Y_1}{G_S} + j \left(1 - \frac{Y_1^2}{G_S^2} \right) \frac{\pi}{2} \frac{(\omega - \omega_0)}{\omega_0} \right] \tag{2}$$

It is assumed that the angular frequency (ω) is close to ω_0 . Similarly, the input admittance of Y_A in Figure 3(a) is obtained as (3):

$$Y_A = \frac{J_{0,1}^2 G_S}{Y_1^2} + jB_a, \tag{3}$$

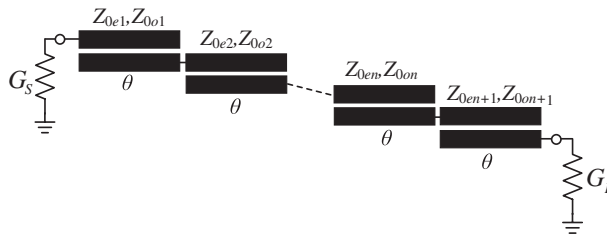


Figure 1. Parallel-couple line bandpass filter.

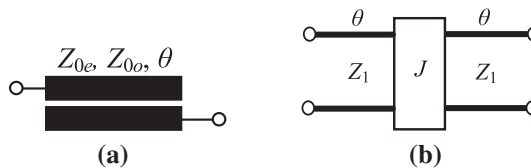


Figure 2. (a) Single parallel-coupled line and (b) its equivalent circuit.

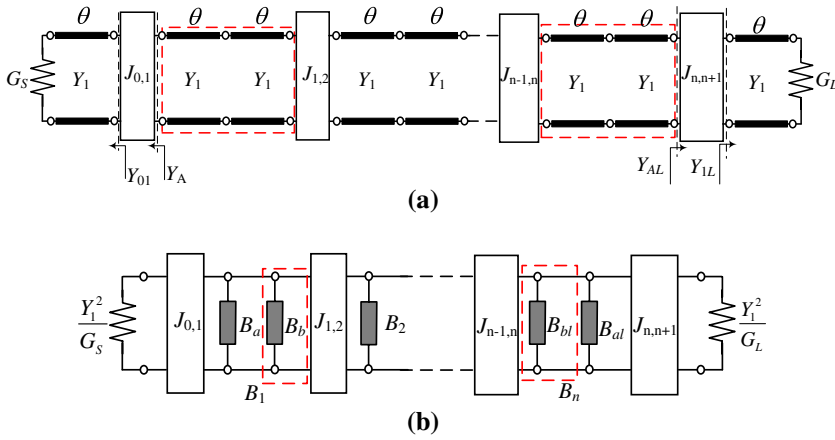


Figure 3. (a) Equivalent circuit of parallel-couple line bandpass filter and (b) modified equivalent circuit model of (a).

where

$$B_a = \frac{J_{0,1}^2}{Y_1} \left(1 - \frac{G_S^2}{Y_1^2} \right) \frac{\pi}{2} \frac{(\omega - \omega_0)}{\omega_0}. \tag{4}$$

B_a is the susceptance of Y_A and it is combined with the first resonator. The real part of Y_A becomes a source termination conductance of a modified equivalent circuit as shown in Figure 3(b). Then, the total susceptance of the first resonator B_1 becomes as:

$$B_1(\omega) = B_a(\omega) + B_b(\omega) \tag{5}$$

where

$$B_b(\omega) = 2Y_1 \frac{\pi}{2} \frac{(\omega - \omega_0)}{\omega_0}. \tag{6}$$

B_b is the susceptance of resonator between inverter $J_{0,1}$ and $J_{1,2}$. From (5), the susceptance slope parameter is derived in (7):

$$b_1 = \frac{\omega_0}{2} \frac{dB_1(\omega)}{d\omega} \Big|_{\omega=\omega_0} = \frac{\pi}{2} \left[\frac{J_{0,1}^2}{2Y_1} \left(1 - \frac{G_S^2}{Y_1^2} \right) + Y_1 \right]. \tag{7}$$

On the other hand, the input admittance (Y_{1L}) looking toward the load is derived in (8):

$$Y_{1L} = Y_1 \frac{G_L + jY_1 \tan \theta}{Y_1 + jG_L \tan \theta} \approx Y_1 \left[\frac{Y_1}{G_L} + j \left(1 - \frac{Y_1^2}{G_L^2} \right) \frac{\pi}{2} \frac{(\omega - \omega_0)}{\omega_0} \right] \tag{8}$$

Similarly, the input admittance Y_{AL} in Figure 3(a) is given as (9):

$$Y_{AL} = \frac{J_{n,n+1}^2 G_L}{Y_1^2} + jB_{al}, \tag{9}$$

where

$$B_{al} = \frac{J_{n,n+1}^2}{Y_1} \left(1 - \frac{G_L^2}{Y_1^2} \right) \frac{\pi}{2} \frac{(\omega - \omega_0)}{\omega_0}. \tag{10}$$

In this case, B_{al} is the susceptance of Y_{AL} and it is combined with the last resonator. The real part of Y_{AL} becomes a load termination conductance of a modified equivalent circuit as shown in Figure 3(b). Then, total susceptance of the last resonator B_n becomes as:

$$B_n(\omega) = B_{al}(\omega) + B_{bl}(\omega) \tag{11}$$

where $B_{bl}(\omega) = B_b(\omega)$ is the susceptance of the resonator between inverter $J_{n-1,n}$ and $J_{n,n+1}$. From (11), the slope parameter of the last resonator is computed as (12):

$$b_n = \frac{\omega_0}{2} \left. \frac{dB_n(\omega)}{d\omega} \right|_{\omega=\omega_0} = \frac{\pi}{2} \left[\frac{J_{n,n+1}^2}{2Y_1} \left(1 - \frac{G_L^2}{Y_1^2} \right) + Y_1 \right]. \tag{12}$$

Beside the first and last susceptance resonators, the susceptances of the intermediate resonators are equal to B_b and their slope parameters [28] are obtained as (13):

$$b_i = \frac{\omega_0}{2} \left. \frac{dB_b(\omega)}{d\omega} \right|_{\omega=\omega_0} = \frac{\pi}{2} Y_1 \quad i = 2, 3, \dots, n - 1. \tag{13}$$

Then, the design formulas of J -inverters with arbitrary termination impedances and image admittance (Y_1) are calculated as (14):

$$J_{0,1} = Y_1 \sqrt{\frac{\frac{Y_1}{G_s} \frac{\pi}{2} FBW}{g_0 g_1 - \frac{\pi}{4} \left(\frac{Y_1}{G_s} - \frac{G_s}{Y_1} \right) FBW}}, \tag{14a}$$

$$J_{1,2} = FBW \sqrt{\frac{b_1 b_2}{g_1 g_2}}, \tag{14b}$$

$$J_{i-1,i} = FBW \sqrt{\frac{b_{i-1} b_i}{g_{i-1} g_i}}, \quad i = 3, 4, \dots, n - 1 \tag{14c}$$

$$J_{n-1,n} = FBW \sqrt{\frac{b_{n-1} b_n}{g_{n-1} g_n}}, \tag{14d}$$

$$J_{n,n+1} = Y_1 \sqrt{\frac{\frac{Y_1}{G_L} \frac{\pi}{2} FBW}{g_n g_{n+1} - \frac{\pi}{4} \left(\frac{Y_1}{G_L} - \frac{G_L}{Y_1} \right) FBW}}, \tag{14e}$$

where g_0, g_1, \dots, g_{n+1} are the prototype low-pass element values, which can be computed for either Butterworth or Chebyshev responses [28]. FBW is the fractional bandwidth of the passband. b_1, b_n , and b_i are calculated from (7), (12), and (13), respectively.

In case of $n = 2$, the first and last J -inverters are the same for (14a) and (14e), respectively; however, the $J_{1,2}$ is found as (15):

$$J_{1,2} = FBW \sqrt{\frac{b_1 b_n}{g_1 g_2}} \tag{15}$$

where n is number of stages. From (14) to (15), the J -inverter values can be calculated for either Butterworth or Chebyshev responses with arbitrary real termination and image impedances of parallel-coupled lines. Then, the even- and odd-mode characteristic impedances of parallel-coupled lines are computed using (1).

3. Design examples

The design procedures of proposed filter are summarized with design flowchart as shown in Figure 4.

Design examples including different n , image impedance, and termination impedances are presented to verify the design formulas. The filters are designed for $FBW = 5\%$ and passband ripple (L_{Ar}) of 0.0434 dB ($S_{11} = -20$ dB). Using the above design steps, the calculated circuit parameters with the Chebyshev response are given in Table 1. In these simulations, ideal elements are used in advance design system (ADS) to simulate the theoretical performances of the proposed BPF.

Figure 5(a) shows the S -parameter and equal ripple characteristics with different n . As shown in the figure, the numbers of transmission pole are proportional to the n . The stopband attenuation become steeper as the n increases. Moreover, the magnitudes of equal

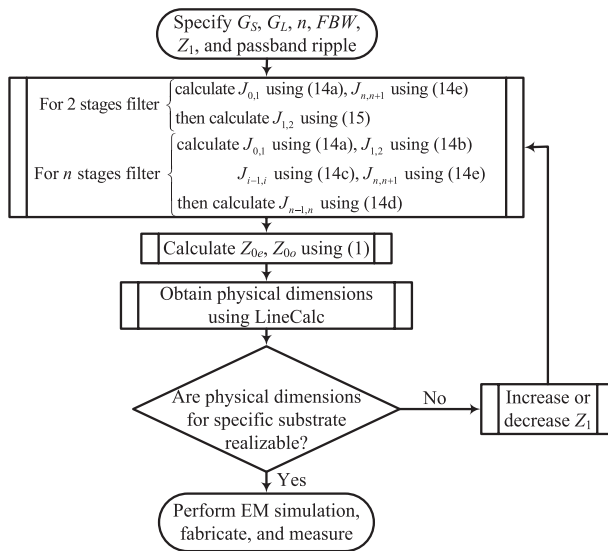


Figure 4. Design flowchart of proposed bandpass filter.

Table 1. Calculated even- and odd-mode characteristic impedances of the coupled line BPF with Chebyshev response.

$f_0 = 2.6 \text{ GHz}, FBW = 5\%, L_{Ar} = 0.0434 \text{ dB}$					
		$R_S = 20 \Omega, R_L = 50 \Omega, Z_1 = 50 \Omega$			n
	62.33/41.86	56.89/44.61	73.05/38.73		2
	60.84/42.52	54.16/46.43	54.37/46.28	69.77/39.43	3
	60.34/42.75	53.66/46.81	52.89/47.4	53.83/46.68	4
		$R_S = 80 \Omega, R_L = 50 \Omega, n = 4$			$Z_1 (\Omega)$
	52.4/22.5	32.43/27.91	31.74/28.44	32.35/27.96	30
	75.75/38.28	53.92/46.61	52.89/47.4	53.83/46.67	50
	98.64/54.97	75.39/65.32	74.06/66.36	75.28/65.41	70
$Z_{oe}/Z_{oo} (\Omega)$		$R_S = 10 \Omega, R_L = 500 \Omega, Z_1 = 60 \Omega$			n
	67.04/54.31	64.09/56.4	63.48/56.88	65.77/55.16	186.41/62.19
		$R_S = 50 \Omega, R_L = 50 \Omega, Z_1 = 60 \Omega$			
	79.91/48.37	64.56/56.04	63.48/56.88	64.56/56.04	79.91/48.37
		$R_S = 30 \Omega, R_L = 90 \Omega, Z_1 = 60 \Omega$			
	74.31/50.44	64.45/56.13	63.48/56.88	64.68/55.95	89.55/46.15

ripples are maintained even though n vary from 2 to 4 and R_S is not 50 Ω . Figure 5(b) shows the S -parameter and passband ripple characteristics with different Z_1 . The S -parameter characteristics and equal ripples are maintained for all Z_1 ; therefore, the changing Z_1 does not affect the filter response. Figure 5(c) shows the S -parameter and passband ripples characteristics with different r . r is defined as the ratio of source to load termination impedances ($r = R_S/R_L$). The passband characteristics were still maintained with the changing r ; however, the stopband attenuation is more attenuated when the r is very small.

4. Measurement results

For the experimental validation, two BPFs with different termination impedances and n were designed, simulated, and fabricated at center frequency (f_0) of 2.6 GHz. The filter 1 is designed with $R_S = 50 \Omega, R_L = 300 \Omega, n = 2, Z_1 = 60 \Omega, FBW = 5\%$, and $L_{Ar} = 0.0434 \text{ dB}$. The calculated element values of filter 1 are $Z_{oe1} = 84.36 \Omega, Z_{oo1} = 47.17 \Omega, Z_{oe2} = 70.52 \Omega, Z_{oo2} = 52.26 \Omega, Z_{oe3} = 163.64 \Omega$, and $Z_{oo3} = 54.9 \Omega$. The filter 2 is designed with $R_S = 20 \Omega, R_L = 50 \Omega, n = 3$, and FBW and ripple are the same as those of filter 1. The calculated element values are already shown in Tables 1. The proposed circuits were fabricated on an RT/Duroid 5880 substrate with a dielectric constant (ϵ_r) of 2.2 and a thickness (h) of 0.787 mm. The width, spacing, and length of resonators were calculated using LineCalc of ADS tool. The EM simulation was performed using the ANSYS HFSS.

The layout and fabricated circuit of filter 1 are displayed in Figure 6. Fabrication data are listed in Table 2. The simulated and measured results of narrow and broadband characteristics are plotted in Figure 7(a) and (b), respectively, where the measured center frequency is the same as those of simulated. The measured passband insertion and input/output return losses are better than 0.8 and 19.6 dB, respectively. The spurious response was produced in the stopband due to the difference between the even- and odd-mode phase velocities of coupled microstrips [29,30].

Figure 8 shows the layout and a photograph of fabricated filter 2 in microstrip line. Fabrication data are listed in Table 3. The simulated and measured S -parameters of proposed

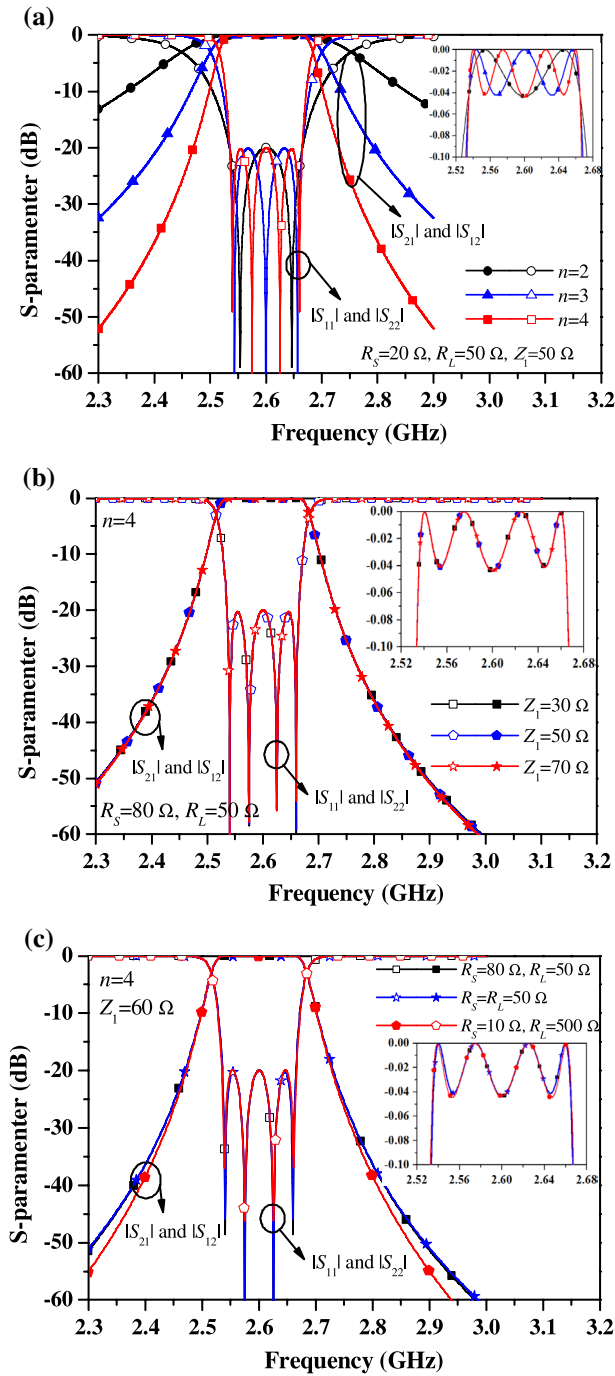


Figure 5. S-parameters characteristics of proposed BPF with different: (a) n , (b) Z_1 , and (c) r .

filter are shown in Figure 9(a) and (b) for narrow and broadband characteristic, respectively. The measured results are agreed well with those of simulated results. The measured insertion and input/output return losses are better than 1.5 and 19 dB within the passband frequency

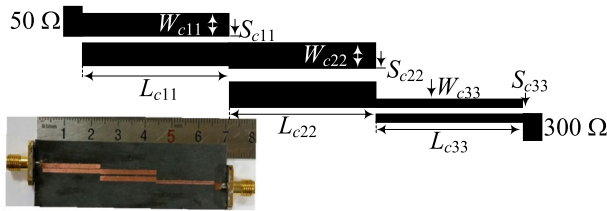


Figure 6. Layout and photograph of the fabricated bandpass filter 1.

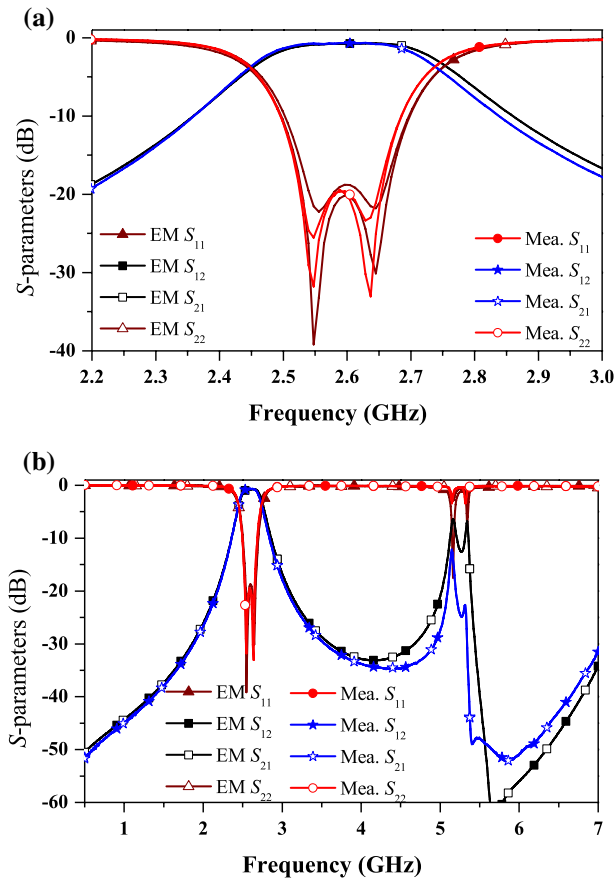


Figure 7. Simulated and measured results of filter 1: (a) narrow band and (b) broadband characteristics.

Table 2. Physical dimensions of the fabricated bandpass filter 1. (unit: mm).

$W_{c11} = 1.46$	$W_{c22} = 1.69$	$W_{c33} = 0.4$
$S_{c11} = 0.25$	$S_{c22} = 0.75$	$S_{c33} = 0.2$
$L_{c11} = 20.9$	$L_{c22} = 20.9$	$L_{c33} = 21.4$

of 2.527 to 2.667 GHz ($FBW = 5.3\%$), respectively. The stopband attenuation is better than 23 dB of the lower stopband from DC to 2.37 GHz and the higher stopband from 2.8 to 7 GHz.

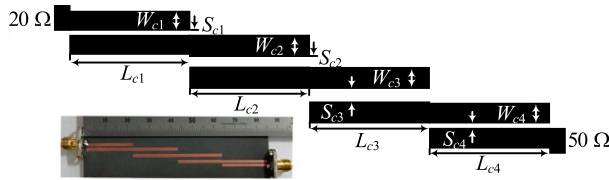


Figure 8. Layout and photograph of the fabricated bandpass filter 2.

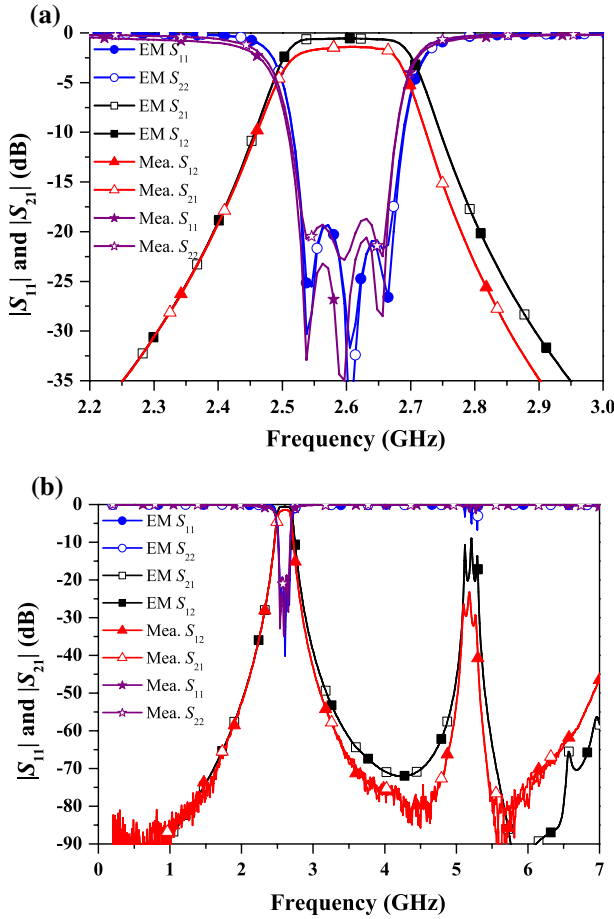


Figure 9. Simulated and measured results of the filter 2: (a) narrow band and (b) broadband characteristics.

Table 3. Physical dimensions of the fabricated bandpass filter 2. (unit: mm).

$W_{e1} = 1.55$	$W_{e2} = 1.63$	$W_{e3} = 1.6$	$W_{e4} = 1.4$
$S_{e1} = 0.65$	$S_{e2} = 1.4$	$S_{e3} = 1.38$	$S_{e4} = 0.35$
$L_{e1} = 21$	$L_{e2} = 21$	$L_{e3} = 20.75$	$L_{e4} = 21.15$

The performance comparison of the parallel-coupled line BPFs and ITs are summarized in Table 4. The proposed BPF has merits on the numbers of filter stages and arbitrary termination impedances with high r when compared with others. The structure of the proposed

Table 4. Performances comparison with previous works related to parallel-coupled lines bandpass filter.

Ref.	f_0 (GHz)	R_S-R_L	n	Design equations	r	Image impedance
[1]	1.2	50–50	i	Analytical	1	NA
[2]	1.85	50–50	i	Analytical	1	Arbitrary
[3]	NA	50–50	i	Analytical	1	Arbitrary
[4]	1.85	50–50	3	Analytical	1	Arbitrary
[5]	0.9	50–50	i	Analytical	1	NA
[6]	2.45	50–50	9	Analytical	1	NA
[13]	2	Arbitrary	1	analytical	Low	Arbitrary
[14]	2.6	Arbitrary	1	Analytical	Medium	Arbitrary
[19]	2.6	Arbitrary	2	Analytical	High	Arbitrary
[20]	3	Arbitrary	i	Optimization	Low	NA
This work	2.6	Arbitrary	i	Analytical	High	Arbitrary

$i = 2 \text{ to } n + 1$

BPF is comparable with that of [20]; however, the new design formulas have been derived for more general, accurate values, and high r . The derived formulas are more advantageous and easy to use for the higher stage filters and various r values. Also, the image impedance of coupled line might be chosen arbitrary for the design convenience.

5. Conclusion

This paper has presented an innovative design theory of parallel-coupled line bandpass filters with arbitrary real termination and image impedances. The design formulas for the proposed filter have been derived using coupled line filter theory. To show the validity of the proposed design formulas, two parallel-coupled line BPFs are fabricated and measured with Chebyshev responses. The simulated and measured results are agreed well with the analysis. The derived formulas are applicable in many applications such as power divider, matching network, and power amplifier design with many design advantages. In the future work, a wideband BPF with unequal termination impedance is going to study.

Disclosure statement

No potential conflict of interest was reported by the authors.

Funding

This research was supported by the Basic Science Research Program through the National Research Foundation of Korea (NRF) funded by the Ministry of Education, Science and Technology [2016R1D1A1B03931400]; and partially supported by Korean Research Fellowship Program through the National Research Foundation of Korea (NRF) funded by ministry of Science and ICT [2016H1D3A1938065].

ORCID

Phirun Kim  <http://orcid.org/0000-0002-3889-8253>

Girdhari Chaudhary  <http://orcid.org/0000-0003-2060-9860>

Yongchae Jeong  <http://orcid.org/0000-0001-8778-5776>

References

- [1] Cohn SB. Parallel-coupled transmission-line-resonator filters. *IRE Trans Microw Theory Tech.* 1958;6:223–231.
- [2] Ahn D, Kim C, Chung M, et al. The design of Parallel coupled line filter with arbitrary image impedance. *IEEE Intern Microw Symp Digest.* 1998;2:909–912.
- [3] Swanson D, Macchiarella G. Microwave filter design by synthesis and optimization. *IEEE Microw Magaz.* 2007;8:55–69.
- [4] Park J, Yun J, Ahn D. A design of the novel coupled-line bandpass filter using defected ground structure with wide stopband performance. *IEEE Trans Microw Theory Tech.* 2002;50:2037–2043.
- [5] Cheong P, Fok S, Tam K. Miniaturized parallel coupled-line bandpass filter with spurious-response suppression. *IEEE Trans. Microw. Theory Tech.* 2005;53:1810–1816.
- [6] Chin K, Chiou Y, Kuo J. New synthesis of parallel-coupled line bandpass filter with Chebyshev responses. *IEEE Trans Microw Theory Tech.* 2008;56:1516–1523.
- [7] Zhang S, Zhu L. Synthesis method for even-order symmetrical Chebyshev bandpass filters with alternative inverters and resonators. *IEEE Trans Microw Theory Tech.* 2013;61:808–816.
- [8] Wu Y, Cui L, Zhang W, et al. High performance single-ended wideband and balance bandpass filters loaded with stepped-impedance stubs. *IEEE Access.* 2017;5:5972–5981.
- [9] Wu Y, Chen Y, Jiao L, et al. Dual-band dual-mode substrate integrated waveguide filters with independently reconfigurable TE₁₀₁ resonant mode. *Sci Rep.* 2016;6:1–10.
- [10] Wu Y, Cui L, Zhuang Z, et al. A simple planar dual-band bandpass filter with multiple transmission poles and zeros. *IEEE Trans Circuits Syst II: Express Briefs.* 2017. DOI:10.1109/TCSII.2017.2702191
- [11] Levy R. Synthesis of mixed lumped and distributed impedance-transforming filters. *IEEE Trans Microw Theory Tech.* 1972;20:223–233.
- [12] Kim P, Chaudhary G, Jeong Y. Wideband impedance transformer with out-of-band suppression characteristics. *Microw Opt Techno Lett.* 2014;56:2612–2616.
- [13] Ahn H, Itoh T. Impedance-transforming symmetric and asymmetric DC blocks. *IEEE Trans Microw Theory Tech.* 2010;58:2463–2474.
- [14] Kim P, Chaudhary G, Jeong Y. Enhancement impedance transforming ratios of coupled line impedance transformer with wide out-of-band suppression characteristics. *Microw Opt Techno Lett.* 2015;57:1600–1603.
- [15] Kim P, Jeong Y, Chaudhary G, et al. A design of unequal termination impedance power divider with filtering and out-of-band suppression characteristics. *Proceedings of the 45th European Microwave Conference; Paris; 2015.* p. 123–126.
- [16] Jeong J, Kim P, Jeong Y. High efficiency power amplifier with frequency band selective matching networks. *Microw Opt Techno Lett.* 2015;57:2031–2034.
- [17] Wu Y, Zhuang Z, Yan G, et al. Generalized dual-band unequal filtering power divider with independently controllable bandwidth. *IEEE Trans Microw Theory Tech.* 2017;65:3838–3848.
- [18] Chen W-K. *Theory and design of broadband matching networks.* Oxford: Pergamon; 1976.
- [19] Kim P, Chaudhary G, Jeong Y. Ultra-high transforming ratio coupled line impedance transformer with bandpass response. *IEEE Microw Wireless Comp Lett.* 2015;25:445–447.
- [20] Oraizi H, Moradian M, Hirasawa K. Design and optimization of microstrip parallel-coupled line bandpass filters incorporating impedance matching. *IEICE Trans Commun.* 2006;E89-B:2982–2988.
- [21] Chen K, Peroulis D. Design of broadband highly efficient harmonic tuned power amplifier using in-band continuous Class-F⁻¹/F mode transferring. *IEEE Trans Microw Theory Tech.* 2012;60:4107–4116.
- [22] Matthaei GL. Tables of Chebyshev impedance-transformation networks of low-pass filter form. *Proc IEEE.* 1964;52:939–963.
- [23] Chen K, Liu X, Chappell W, et al. Co-design of power amplifier and narrowband filter using high-Q evanescent-mode cavity resonator as the output matching network. *IEEE Int Microw Symp Digest.* 2011:1–4.
- [24] Chen K, Lee J, Chappell W, et al. Co-design of highly efficient power amplifier and high-Q output bandpass filter. *IEEE Trans Microw Theory Tech.* 2013;61:3940–3950.

- [25] Chen K, Lee T, Peroulis D. Co-design of multi-band high-efficient power amplifier and three-pole high-Q tunable filter. *IEEE Microw Wireless Comp Lett.* [2013](#);23:647–649.
- [26] Ge C, Zhu X, Jiang X, et al. A general synthesis approach of coupling matrix with arbitrary reference impedances. *IEEE Microw Wireless Comp Lett.* [2015](#);25:349–351.
- [27] Jarry P, Beneat J. *Advanced design techniques and realizations of microwave and RF filters.* Wiley; [2008](#).
- [28] Matthaei GL, Young L, Jones EMT. *Microwave filter, impedance-matching networks, and coupling structures.* New York (NY): McGraw-Hill; [1964](#).
- [29] Chin K, Kuo J. Insertion loss function synthesis of maximally flat parallel-coupled line bandpass filters. *IEEE Trans Microw Theory Tech.* [2005](#);53:3161–3168.
- [30] James PG, Constantine Balanis A. Pulse Distortion on multilayer coupled microstrip line. *IEEE Trans Microw Theory Tech.* [1998](#);37:1620–1628.